Characterizing the Distribution of Completion Shapes with Corners Using a Mixture of Random Processes

Karvel K. Thornber

NEC Research Institute
4 Independence Way
Princeton, NJ 08540

Lance R. Williams

Dept. of Computer Science
University of New Mexico
Albuquerque, NM 87131

October 31, 1998

Abstract

We derive an analytic expression for the distribution of contours $\mathbf{x}(t)$ generated by fluctuations in $\dot{\mathbf{x}}(t) = \partial\mathbf{x}(t)/\partial t$ due to random impulses of two limiting types. The first type are frequent but weak while the second are infrequent but strong. The result has applications in computational theories of figural completion and illusory contours because it can be used to model the prior probability distribution of short, smooth completion shapes punctuated by occasional discontinuities in orientation (i.e., corners). This work extends our previous work on characterizing the distribution of completion shapes which dealt only with the case of frequently acting weak impulses.

1 Introduction

In a previous paper[1] we derived an analytic expression characterizing a distribution of short, smooth contours. This result has applications in ongoing work on figural completion[2] and perceptual saliency[3]. The idea that the prior probability distribution of boundary completion shapes can be characterized by a directional random walk is first described by Mumford[4]. A similiar idea is implicit in Cox *et al.*'s use of the Kalman filter in their work on grouping of contour fragments[5]. More recently, Williams and Jacobs[6] introduced a representation they called a *stochastic completion field*—the probability that a particle undergoing a directional random walk will pass through any given position and orientation in the image plane on a path bridging a pair of boundary fragments. They argued that the mode, magnitude and variance of the stochastic completion field are related to the perceived shape, salience and sharpness of illusory contours.

Both Mumford[4] and Williams and Jacobs[6] show that the maximum likelihood path followed by a particle undergoing a directional random walk between two positions and

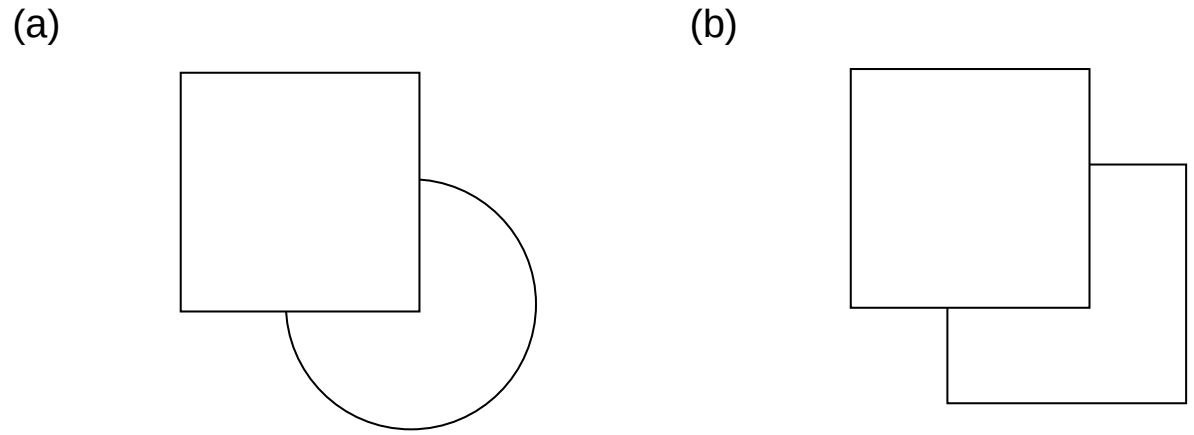

Figure 1: Amodal completion of a partially occluded circle and square (redrawn from Kanizsa[9]). In both cases, completion is accomplished in a manner which preserves tangent and curvature continuity at the ends of the occluded boundaries.

directions is a curve of least energy (see Horn[7]). This is the curve that is commonly assumed to model the shape of illusory contours, and is widely used for semi-automatic region segmentation in many computer vision applications (see Kass *et al.*[8]).

The distribution of shapes considered by [1, 4, 5, 6] basically consists of smooth, short contours. Yet there are many examples in human vision where completion shapes perceived by humans contain discontinuities in orientation (i.e., corners). Figure 1 shows a display by Kanizsa[9]. This display illustrates the completion of a circle and square under a square occluder. The completion of the square is significant because it includes a discontinuity in orientation. Figure 2 shows a pair of "Koffka Crosses." When the width of the arms of the Koffka Cross is increased, observers generally report that the percept changes from an illusory circle to an illusory square[10].

Although the distribution of completion shapes with corners has not previously been characterized analytically, the idea of including corners in completion shapes is not new. For example, the functionals of Kass *et al.*[8] and Mumford and Shah[11] permit orientation discontinuities accompanied by large (but fixed size) penalties. This follows work by Blake[12] and others[13, 14, 15, 16] on interpolation of smooth surfaces with creases from sparse depth (or brightness) measurements. More recently, Belheumer[17] (working with stereo pairs) used a similiar functional for interpolation of disparity along epipolar lines. Belheumer's approach is especially related because he derives his functional by considering a distribution of surface cross-section shapes characterized by a mixture of random processes—smoothly varying disparity is modeled by a one-dimensional Brownian motion while depth discontinuities are modeled by a Poisson process.

In this paper, we derive a very general integral-differential equation underlying a family of contour shape distributions. This family is based on shapes traced by particles following any of several default paths modified by random impulses drawn from a mixture of distributions

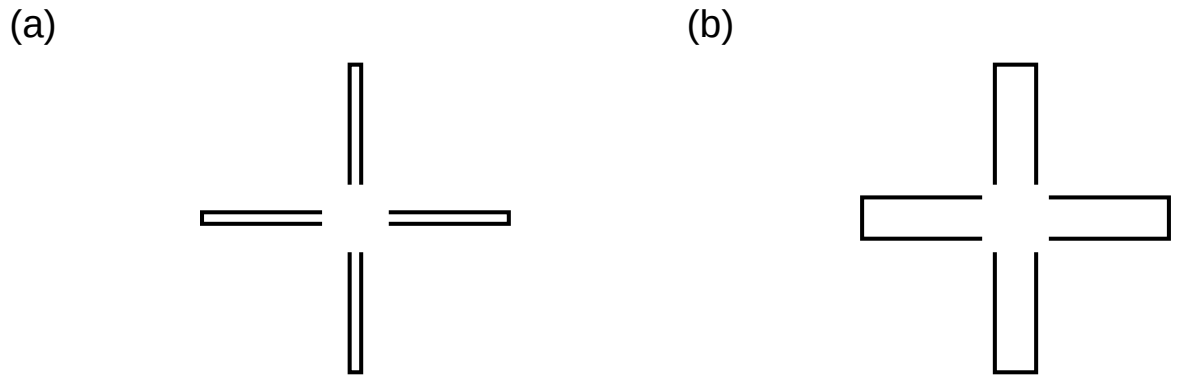

Figure 2: When the width of the arms of the Koffka Cross is increased, observers generally report that the percept changes from an illusory circle to an illusory square (see [2]).

(e.g., different magnitudes, directions, rates). For our figural completion application, we are especially interested in a shape distribution based upon straight line base-trajectories in two-dimensions modified by random impulses drawn from a mixture of two limiting distributions. The first distribution consists of weak but frequently acting impulses (we call this the Gaussian-limit). The distribution of these weak random impulses has zero mean and variance equal to σ_g^2. The weak impulses act at Poisson times with rate R_g. The second consists of strong but infrequently acting impulses (we call this the Poisson-limit). The distribution of these strong random impulses has zero mean and variance equal to σ_p^2 (where $\sigma_p^2 >> \sigma_g^2$). The strong impulses act at Poisson times with rate $R_p << R_g$. As in our previous work, particles decay at an average rate of $1/\tau$. The distribution can be summarized by four parameters which are of constant value for a given application.[1] The effect is that particles tend to travel in smooth, short paths punctuated by occasional orientation discontinuities.

2 Approach

Suppose we are given a collection of contour segments, for example, as would be present in an image of objects occluded by other objects. Our goal is to predict all reasonably likely completions of these contours and their relative likelihoods. If $\mathbf{x}_1$ is the location of the end of one contour segment, and $\mathbf{x}_2$ is the beginning of another, then one candidate for the most general prior between $\mathbf{x}_1$ and $\mathbf{x}_2$ would be given by:

$$\mathbf{x}(t) = \mathbf{x}_1 + \sum_\ell \Delta\mathbf{x}_\ell u(t - t_\ell), \quad t_1 < t_i < t_2, \quad \mathbf{x}(t_2) = \mathbf{x}_2$$

where $u(\cdot)$ is the unit step function, i.e., $u(t) = 0$ when $t < 0$ and $u(t) = 1$ when $t > 0$ and the displacements $\Delta\mathbf{x}_\ell$ are stochastic with some zero-mean distribution. The times t_ℓ

[1] There are four (not five) because we combine σ_g^2 and R_g into a single parameter, $T = R_g\sigma_g^2$.

would also be stochastic, e.g., Poisson with some (possibly time varying) rate $\mathbf{R}(t)$. Such curves would resemble the tracks of classical Brownian particles connecting $\mathbf{x}_1$ and $\mathbf{x}_2$. While this represents the most general prior for a continuous curve, lacking any bias, the expected contour will be simply

$$< \mathbf{x}(t) >= \mathbf{x}_1 + \mathbf{x}_2(t - t_1)/(t_2 - t_1), \quad t_1 \leq t \leq t_2$$

which in space is independent of t_1 and t_2, and the details of the distribution of the $(\Delta\mathbf{x}_\ell, t_\ell)$. For ordinary diffusion in one and two dimensions, all points can be reached with probability one. For this reason, such completions are both degenerate and sterile, and will not be considered further.

Except at isolated points (corners), most boundaries are continuous in position and orientation. Thus, if in the above example, θ_1 and θ_2 are the directions at $\mathbf{x}_1$ and $\mathbf{x}_2$, then two additional boundary conditions enter:

$$d\mathbf{x}/ds = [\cos\theta_1, \sin\theta_1] \text{ at } \mathbf{x}_1 \text{ and } d\mathbf{x}/ds = [\cos\theta_2, \sin\theta_2] \text{ at } \mathbf{x}_2$$

where s is the distance along the curve $\mathbf{x}$(s) as in differential geometry. Between $\mathbf{x}_1$ and $\mathbf{x}_2$ one would like to write $d\mathbf{x}/ds = [\cos\theta(s), \sin\theta(s)]$ where $\dot{\theta}(s)$ is a normally distributed random variable with zero mean (i.e., $\theta(s)$ is a Brownian motion). See Mumford[4] and Williams and Jacobs[6]. Note that speed is assumed to be constant. In this paper, we consider more general contours $\mathbf{x}(t)$ with arbitrary parameterization (t), and for each component q, set

$$dx_q(t)/dt = \dot{x}_q(t), \quad q = 1, ..., d$$

where the $\dot{x}_q(t)$ are independent random variables. Each $\dot{x}_q$ changes by $\Delta\dot{x}_{q\ell}$ at $t_{q\ell}$ according to a zero-mean distribution on $\Delta\dot{x}_q$, while the $t_{q\ell}$ occur at a mean rate of $R_q(t)$, for example, according to Poisson statistics. This results in what is probably the least constrained, simple prior which captures the essential properties of the missing contour and its relative likelihood:

$$\mathbf{x}(t) = \mathbf{x}_1 + \dot{\mathbf{x}}_1(t - t_1) + \int_{t_1}^{t} dt' \sum_\ell \Delta\dot{\mathbf{x}}_\ell u(t' - t_\ell), \quad t_1 \leq t' \leq t_2$$

where $\mathbf{x}(t_2) = \mathbf{x}_2, \dot{\mathbf{x}}(t_2) = \dot{\mathbf{x}}_2$. [2] Clearly $\dot{\mathbf{x}}_1$ and $\dot{\mathbf{x}}_2$ will have directions θ_1 and θ_2.

3 Prior Distribution of Smooth Completion Shapes

We define $P(2 \mid 1)$ to be the likelihood that a contour, $\mathbf{x}(t)$, is at $\mathbf{x}_2$ with $\dot{\mathbf{x}}_2$ for $t = t_2$ given that it was at $\mathbf{x}_1$ with $\dot{\mathbf{x}}_1$ for $t = t_1$, averaged over all $\mathbf{x}(t)$ subjected to random impulses. While we calculate $P(2 \mid 1)$ directly in the next section (for a mixture of frequent-weak impulses and infrequent-strong impulses), it is of value to derive an integral-differential equation for $P(2 \mid 1)$ which includes all types of impulses.

[2] More generally, and for those who eschew abruptness, we will broaden the $\Delta\dot{\mathbf{x}}_\ell$ impulses by employing a stochastic "force" of the form $\mathbf{F}_t = \sum_\ell \mathbf{f}(t - t_\ell)$, where the $\mathbf{f}(\cdot)$ are "smooth" functions of t.

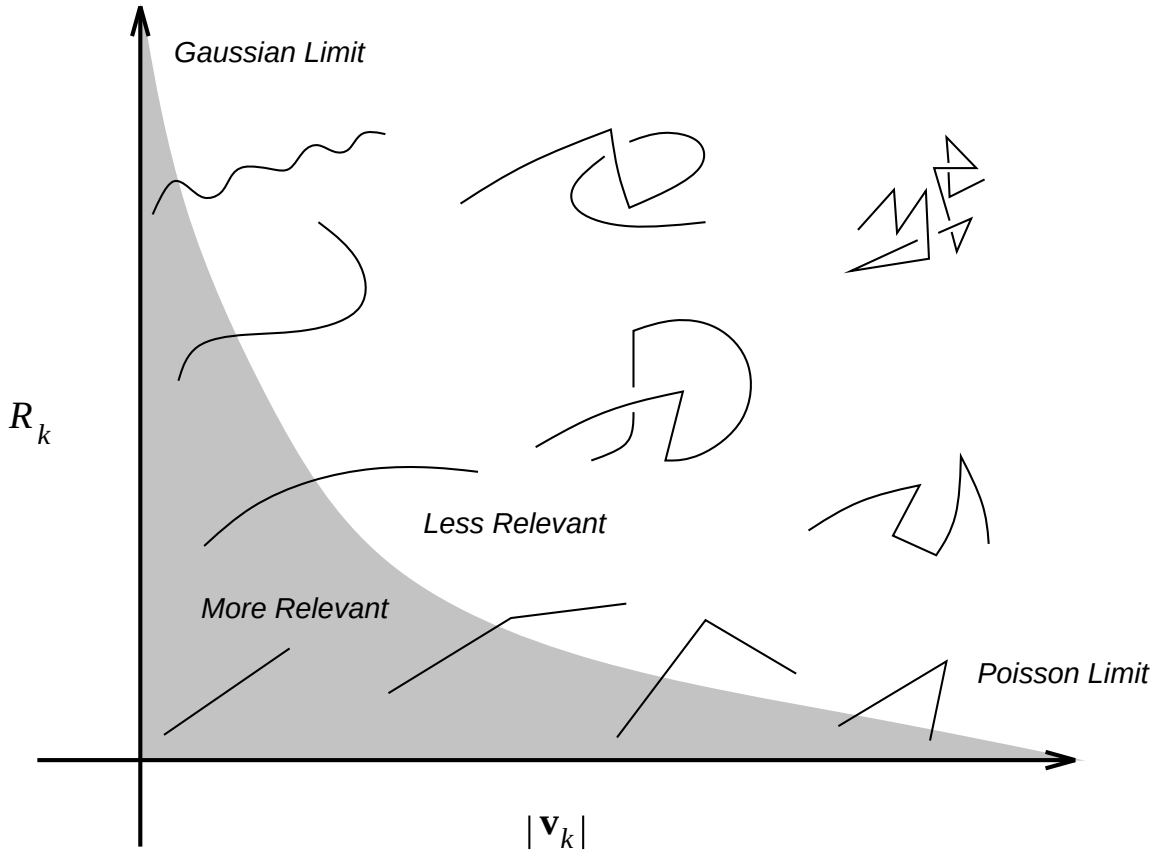

Figure 3: Examples of stochastic curves for various impulse rates, R_k, and impulse magnitudes, $|\mathbf{v}_k|$. The most relevant region of this shape space is spanned by a mixture of frequent-weak (Gaussian) and infrequent-strong (Poisson) processes.

The transition probability, $P(2 \mid 1)$, embodies three aspects of contour distributions: 1) boundary conditions; 2) base-trajectories; and 3) impulse statistics. Boundary conditions constrain possible contours at keypoints[3] by specifying at least one of $\mathbf{x}_i, \dot{\mathbf{x}}_i, \ddot{\mathbf{x}}_i$, etc. We find the choice of $(\mathbf{x}_i, \dot{\mathbf{x}}_i)$ to be most useful, but other applications may require other combinations. A variety of base-trajectories can represent the contour at times between the arrival of random impulses. We have found straight lines to be the most useful in our application. In addition to boundary conditions and base-trajectories, the contour distributions are defined by impulse statistics. Random impulses have the form, $\dot{\mathbf{x}}(t) = \sum_{k\ell} \mathbf{v}_k u(t - t_{k\ell})$, which includes process, k, with impulses, $\mathbf{v}_k$, occuring at Poisson distributed times, $t_{k\ell}$, with mean rate, $R_k(t)$. While we focus here on only two processes, frequent-weak (Gaussian) and infrequent-strong (Poisson), an entire spectrum between these limits is also available (see Figure 3).

We now turn to the calculation of an integral-differential equation for $P(2 \mid 1)$. Recall

[3]We use this term (adopted from [18]) as a generic term to denote position-velocity constraints derived from the image.

that $P(2 \mid 1)$ is the probability that given $\mathbf{x}(t_1) = \mathbf{x}_1$ and $\dot{\mathbf{x}}(t_1) = \dot{\mathbf{x}}_1$, then $\mathbf{x}(t_2) = \mathbf{x}_2$ and $\dot{\mathbf{x}}(t_2) = \dot{\mathbf{x}}_2$ for $t_2 > t_1$:

$$\begin{aligned} P(2 \mid 1) &\equiv P(\mathbf{x}_2, \dot{\mathbf{x}}_2, t_2 \mid \mathbf{x}_1, \dot{\mathbf{x}}_1, t_1) \\ &= < \delta(\mathbf{x}(t_2) - \mathbf{x}_2)\delta(\dot{\mathbf{x}}(t_2) - \dot{\mathbf{x}}_2) >_1 \end{aligned}$$

where $< \cdot >_1$ is an average over all contours matching the boundary condition $\mathbf{x}_1, \dot{\mathbf{x}}_1$ at t_1. For conciseness, in the following expressions we write $P(\mathbf{x}, \dot{\mathbf{x}}, t)$ instead of $P(\mathbf{x}_2, \dot{\mathbf{x}}_2, t_2 \mid \mathbf{x}_1, \dot{\mathbf{x}}_1, t_1)$. In these expressions, $(\mathbf{x}, \dot{\mathbf{x}})$ refers to $(\mathbf{x}_2, \dot{\mathbf{x}}_2)$, and the boundary conditions, $(\mathbf{x}_1, \dot{\mathbf{x}}_1)$, are implicit. We find (using $\delta'(t) = \partial\delta(t)/\partial t$):

$$\partial_t P(\mathbf{x}, \dot{\mathbf{x}}, t) = < \dot{\mathbf{x}}_t \delta'(\mathbf{x}_t - \mathbf{x})\delta(\dot{\mathbf{x}}_t - \dot{\mathbf{x}}) >_1 + < \ddot{\mathbf{x}}_t \delta(\mathbf{x}_t - \mathbf{x})\delta'(\dot{\mathbf{x}}_t - \dot{\mathbf{x}}) >_1$$

$$= -\dot{\mathbf{x}} \cdot \partial_{\mathbf{x}} < \delta(\mathbf{x}_t - \mathbf{x})\delta(\dot{\mathbf{x}}_t - \dot{\mathbf{x}}) >_1 - \partial_{\dot{\mathbf{x}}} < \ddot{\mathbf{x}}_t \delta(\mathbf{x}_t - \mathbf{x})\delta(\dot{\mathbf{x}}_t - \dot{\mathbf{x}}) >_1$$

where $\mathbf{x}_t = \mathbf{x}(t)$, $\dot{\mathbf{x}}_t = \dot{\mathbf{x}}(t)$ and $\ddot{\mathbf{x}}_t = \ddot{\mathbf{x}}(t)$. While the delta function, $\delta(\dot{\mathbf{x}}_t - \dot{\mathbf{x}})$, forces the first expectation value to be $\dot{\mathbf{x}}$, the second expectation value is less readily specifiable.[4] From the form and distribution of the random impulses, it follows that $\ddot{\mathbf{x}}_t = \sum_{k\ell} \mathbf{v}_k \delta(t - t_{k\ell})$. As the occurrences of the fluctuations are independent, it is reasonable to take their average instantaneous rate, $R_k(t)$, to be independent of the number of fluctuations, N_k, of type, k, in the interval of interest. This leads us to the standard Poisson distribution for the probability of N_k independent fluctuations, and simplifies the resulting equation. Should this be an over-simplification, we could still work out $P(2 \mid 1)$ as discussed in [1]. These considerations (together with a decay term to reduce the contribution of long contours) result in the following integral-differential equation for $P(\mathbf{x}, \dot{\mathbf{x}}, t)$:

$$\partial_t P(\mathbf{x}, \dot{\mathbf{x}}, t) = -\dot{\mathbf{x}} \cdot \partial_{\mathbf{x}} P(\mathbf{x}, \dot{\mathbf{x}}, t) - \ddot{\mathbf{x}}_{1t} \cdot \partial_{\dot{\mathbf{x}}} P(\mathbf{x}, \dot{\mathbf{x}}, t) - P(\mathbf{x}, \dot{\mathbf{x}}, t)/\tau$$

$$- \sum_k \int d\xi R_k(\xi) \mathbf{f}_k(t - \xi) \cdot \partial_{\dot{\mathbf{x}}} P(\mathbf{x} - \int dt' \mathbf{G}_{t,t'} \mathbf{f}_k(t' - \xi), \dot{\mathbf{x}} - \int dt' \dot{\mathbf{G}}_{t,t'} \mathbf{f}_k(t' - \xi), t)$$

where $\mathbf{x}_{1t}$ is $\mathbf{x}(t)$ for impulse-free conditions, $\mathbf{x}(t_1) = \mathbf{x}_1$ and $\dot{\mathbf{x}}(t_1) = \dot{\mathbf{x}}_1$. For straight line base-trajectories, $\mathbf{G}_{t,t'} = (t^+ - t')u(t^+ - t')\mathbf{I}$ and therefore $\ddot{\mathbf{x}}_{1t} = 0$. This causes the second term to drop out. Then (since the details of the elementary force, $\mathbf{f}_k(t)$, are unlikely to matter) we assume that $\mathbf{v}_k = \int dt\ \mathbf{f}_k(t)$, and obtain:

$$\partial_t P(\mathbf{x}, \dot{\mathbf{x}}, t) = -\dot{\mathbf{x}} \cdot \partial_{\mathbf{x}} P(\mathbf{x}, \dot{\mathbf{x}}, t) - P(\mathbf{x}, \dot{\mathbf{x}}, t)/\tau - \sum_k R_k(t) \mathbf{v}_k \cdot \partial_{\dot{\mathbf{x}}} P(\mathbf{x}, \dot{\mathbf{x}} - \mathbf{v}_k/2, t)$$

The time evolution of the conditional probability at $(\mathbf{x}, \dot{\mathbf{x}})$ is governed by three factors: 1) advection; 2) decay; and 3) diffusion. The effect of the advection term is that probability

[4] In Appendix A we calculate the second expectation value in terms of the probability distribution of the number of times an elementary "force," $\mathbf{f}_k(t - t_{k\ell})$, acts in a given interval of time. Though exact, for our present purposes, the expression is unnecessarily complicated.

mass at $(\mathbf{x}, \dot{\mathbf{x}})$ is transported with velocity $\dot{\mathbf{x}}$. The effect of the decay term is that the total probability mass decreases exponentially with increasing time. It is the diffusion term which is most important. It expresses the fact that the random impulses drive the distribution through its velocity-gradient averaged over the duration of the impulse. In the limit of impulses of short duration, this average can be approximated by the velocity-gradient evaluated at $\dot{\mathbf{x}} - \mathbf{v}_k/2$ (i.e., the average velocity before and after the fluctuation). For small impulses, $\mathbf{v}_k$, and for stationary processes (i.e., for constant R_k), we obtain the following simple differential equation for the conditional probability:

$$\partial_t P_0 = -\dot{\mathbf{x}} \cdot \partial_{\mathbf{x}} P_0 + \mathbf{T}\partial^2_{\dot{\mathbf{x}}} P_0/2 - P_0/\tau, \qquad \mathbf{T} = \sum_k R_k \mathbf{v}_k \mathbf{v}_k$$

which for isotropic impulses, becomes:

$$\partial_t P_0 = -\dot{\mathbf{x}} \cdot \partial_{\mathbf{x}} P_0 + T\partial^2_{\dot{\mathbf{x}}} P_0/2 - P_0/\tau$$

where T is the velocity-variance-rate parameter, analogous to the position-variance-rate parameter (diffusion coefficient) of transport theories.[5] This *Fokker-Planck* equation is similiar to the equation described by Mumford[4]. The only difference is that the diffusion term in our equation involves velocity rather than orientation. One consequence of this difference is that our equation separates, so that $P_0(2 \mid 1) = \exp(-t/\tau) P_{0x}(2 \mid 1) P_{0y}(2 \mid 1)...$, the product extending to as many dimensions as are of interest. Solving, we find for $P_{0x}(2 \mid 1)$:

$$P_{0x}(2 \mid 1; t) = \frac{\exp[-\dot{x}_{21}^2/2Tt]}{\sqrt{2\pi Tt}} \cdot \frac{\exp[-6(x_{21} - v_x t)^2/Tt^3]}{\sqrt{\pi Tt^3/6}}$$

and similarly for y, z, ..., etc. Here $v_x = (\dot{x}_2 + \dot{x}_1)/2$, $t = t_2 - t_1$,$\dot{x}_{21} = \dot{x}_2 - \dot{x}_1$, $x_{21} = x_2 - x_1$, and T arises from setting $T_{ij} = T_i \delta_{ij}$. The expression shows clearly the contribution of velocity diffusion, and the persistence of the initial velocity and anticipation of the final velocity in the position dependence.

4 Inclusion of Corners in Prior Distribution

This formulation is clearly not just limited to frequent-weak impulses—it contains the full spectrum of stochastic contributions to $\dot{\mathbf{x}}_t$. While some problems may call for this flexibility in full, it turns out that corners (discontinuities in orientation) can be included by using a mixture of frequent-weak and infrequent-strong impulses. In fact, for our purposes, it will suffice to include only zero or one large impulse per contour.

[5] In these expressions, the zero subscript denotes the fact that the probability, P_0, is averaged over trajectories modified by zero impulses of the large-infrequent type (i.e., the pure Gaussian case). In the next section, we will consider probabilities averaged over trajectories modified by a mixture of weak, frequent impulses and a single impulse of the large, infrequent type. This mixed probability will be denoted, P_1.

Previously[1] we showed how $P(2 \mid 1) =< \delta(\mathbf{x}(t_2)-\mathbf{x}_2)\delta(\dot{\mathbf{x}}(t_2)-\dot{\mathbf{x}}_2) >_1$ could be obtained from an evaluation of the characteristic functional $\Phi(\mathbf{k}_t) =< \exp i \int dt \mathbf{k}_t \cdot \mathbf{x}_t >_1$ which since

$$\mathbf{x}(t) = \mathbf{x}_1 + \mathbf{G}(t,t_1)\dot{\mathbf{x}}_1 + \int_{t_1}^{t} dt' \mathbf{G}(t,t')\mathbf{F}(t')$$

in which $\mathbf{F}(t')$ is the stochastic force, it sufficed to determine

$$\phi(\mathbf{p}_{t'}) =< \exp(i \int dt' \mathbf{p}_{t'} \mathbf{F}_{t'}) >$$

with $\mathbf{p}_{t'} = \int dt\ \mathbf{k}_t \mathbf{G}(t,t')$ where $\mathbf{G}(t,t') = 0$ for $t \leq t'$. This results in the following expression:

$$< \exp(i \int dt\ \mathbf{p}_t \cdot \mathbf{F}_t) >= \exp[\int d\xi \sum_k R_k(\xi)(\exp(i \int dt\ \mathbf{p}_t\ .\ \mathbf{f}_k(t-\xi)) - 1)]$$

where we used $\mathbf{F}_t = \sum_k \sum_\ell \mathbf{f}_k(t - t_{k\ell})$, the $t_{k\ell}$'s being governed by a Poisson process of rate $R_k(t)$. Although one can use this expression as given (as we do in Appendix A) several limiting cases provide significant and useful simplifications. The most common is the Gaussian limit of small-frequent impulses, which we have already developed, and in which case

$$< \exp(i \int dt\ \mathbf{p}_t \cdot \mathbf{F}_t) >= \exp(-\frac{1}{2} \int dt\ \mathbf{p}_t \cdot \mathbf{T} \cdot \mathbf{p}_t)$$

where $\mathbf{T} = \sum_k R_k \mathbf{v}_k \mathbf{v}_k$ when $\mathbf{f}_k(t) = \mathbf{v}_k \delta(t)$.[6] The opposite limit is large-infrequent impulses. These are necessary if we are to include discontinuities in $d\mathbf{x}(t)/dt$ (i.e., corners). For the case in which a single, large impulse can act in addition to the numerous, small impulses of the Gaussian case, we proceed as follows. Returning to the more general of the above expressions for $< \exp(i \int dt\ \mathbf{p}_t \cdot \mathbf{F}_t) >$, we expand the exponential in $\sum_k R_k(\xi)$ to first order in those processes with low rates, i.e., $\sum_s R_s(\xi)$ where $R_s(\xi)$ is small. In this way, we include only zero and one large scattering events, obtaining the factor:

$$\frac{1 + \sum_s \int d\xi R_s(\xi) \exp[i \int dt\ \mathbf{p}_t \cdot \mathbf{f}_s(t-\xi)]}{1 + \sum_s \int d\xi R_s(\xi)}$$

Again taking the impulses, $\mathbf{f}_s$, to be of relatively short duration and including an average over a Gaussian distribution of variance σ_p^2 (i.e., the least constrained zero-mean distribution of a given variance) we obtain the factor:

$$\frac{1 + \int d\xi R_p(\xi) \exp(-\frac{1}{2}\mathbf{p}_\xi \cdot \sigma_p^2 \cdot \mathbf{p}_\xi)}{1 + \int d\xi R_p(\xi)}$$

normalized to unity for $\mathbf{p}_\xi = 0$ and where $R_p(\xi)$ is the mean rate of this process, i.e., $R_p(\xi) = \sum_s R_s(\xi)$. Here σ_p^2 has the dimensions of (velocity)^2 while $\mathbf{T}$ has the dimensions of (velocity)^2/(time). So finally we find that

$$\phi(\mathbf{p}_t) =< \exp(i \int dt\ \mathbf{p}_t \cdot \mathbf{F}_t) >= \frac{\exp(-\frac{1}{2}\int dt \mathbf{p}_t \cdot \mathbf{T} \cdot \mathbf{p}_t)[1 + \int d\xi R_p(\xi) \exp(-\frac{1}{2}\mathbf{p}_\xi \cdot \sigma_p^2 \cdot \mathbf{p}_\xi)]}{1 + \int d\xi R_p(\xi)}$$

[6] Since the $\mathbf{v}_k$ are small, the exponential in which they occur can be expanded to second order: the zero order term cancels the "–1," and the first order term is zero since the total force has zero mean.

So that the probability of two or more impulses is negligible, it is necessary that $\int d\xi R_p(\xi) << 1$. Using the corresponding result in Appendix A for the Poisson case, we find for $P(2 \mid 1)$ in two dimensions, the expression:

$$P(2\,|\,1;t) = \frac{P_{0x}(2\,|\,1;t)P_{0y}(2\,|\,1;t) + \int_0^t d\xi R_p(\xi) P_{1x}(2\,|\,1;t,\xi) P_{1y}(2\,|\,1;t,\xi)}{1 + \int_0^t d\xi R_p(\xi)} \cdot \exp(-t/\tau)$$

$$P_{1x}(2 \mid 1;t,\xi) = \frac{\exp[-(A_x^2/D + B_x^2/H)/2T]}{2\pi T\sqrt{DH}}$$

$$A_x = x_{21} - \frac{v_x t^2 + \xi_p[\dot{x}_2(t-\xi) + \dot{x}_1\xi]}{t+\xi_p}, \qquad B_x = \dot{x}_{21}$$

$$D = \frac{(t^4/12) + \xi_p(t^3/3 - t^2\xi + \xi^2 t)}{t+\xi_p}, \qquad H = t + \xi_p$$

where $\xi_p = \sigma_p^2/T$ and with analogous expressions for P_{1y}. Note that in the expression for $\phi(\mathbf{p}_t)$, that σ_p^2 is taken to be diagonal. The time, ξ, is the time of the single, large, scattering event. We observe that the Poisson process will dominate for $t << \xi_p$.

The above result for zero and one rare event exhibits several important dependencies. First, recall that T is the velocity-fluctuation rate. Thus, for $Tt < \sigma_p^2$ (i.e., $t < \xi_p$), the frequent-weak process will be less effective than a single strong but rare event. This will be the case for higher velocities (i.e., smaller time intervals). Second, if $R_p(\xi)$ is taken to be a constant, R_p, then $R_p t$ will control the number of rare events (preferably $R_p t << 1$). We note that it would be possible to derive the distribution for one rare event by appropriate joining of two Gaussian processes, but integrals over all intermediate positions *and* velocities would be required.

Although the above expression for $P(2 \mid 1)$ involves a number of symbols, there are in fact only four basic parameters: T, ξ_p, R_p and τ. The values of these four parameters determine the shape distribution and remain constant for a given application. The first parameter, $T = R_g\sigma_g^2$, is the velocity diffusion coefficient.[7] The smaller T becomes, the more the most likely completion will dominate the distribution. Consequently, T controls sharpness. The second parameter, ξ_p, is equal to σ_p^2/T. As mentioned above, if the time associated with the most likely completion is significantly less than ξ_p, then there is not enough time for the frequent-weak impulses to modify the particle's path to match the second boundary condition. Since this factor is in the exponent of the probability expression, infrequent-strong impulses become favored with rate proportional to the third parameter, R_p. Finally, the fourth parameter, τ, determines the rate at which particles decay—the smaller the value of τ, the smaller the contribution of long contours. In practice, we first set T to achieve the desired sharpness in P_0. We then adjust ξ_p to suppress the Gaussian component in P_1 and adjust R_p to achieve the desired mixture of smooth completions and corners.

[7] Ironically, since only the product of R_g and σ_g^2 appears in the equations, in the Gaussian-limit, the distribution of the random impulses, $\mathbf{v}_g$, is arbitrary while in the Poisson-limit, the distribution of the random impulses, $\mathbf{v}_p$, is Gaussian.

5 Sampling and Scale Invariance

Strictly speaking, the above expressions apply only to the continuum. In practice, the expressions must be evaluated on a discrete grid. To reduce aliasing and other artifacts associated with discrete sampling, the transition probabilities can be convolved with broadening functions, for example

$$P(x_2, y_2, \dot{x}_2, \dot{y}_2 \mid x_1, y_1, \dot{x}_1, \dot{y}_1) =$$
$$\int_{-\infty}^{\infty} dx' \int_{-\infty}^{\infty} dy' \int_{-\infty}^{\infty} d\dot{x}' \int_{-\infty}^{\infty} d\dot{y}'\ E(x', \sigma_x^2)\ E(y', \sigma_y^2)\ E(\dot{x}', \sigma_{\dot{x}}^2)\ E(\dot{y}', \sigma_{\dot{y}}^2) \cdot$$
$$p(x_2 - x', y_2 - y', \dot{x}_2 - \dot{x}', \dot{y}_2 - \dot{y}' \mid x_1, y_1, \dot{x}_1, \dot{y}_1)$$

where $E(r', \sigma_r^2) = \exp[-(r'^{\,2}/2\sigma_r^2)]/\sqrt{2\pi\sigma_r^2}$.

In addition to sampling, a second consideration is scale-invariance. Ideally, the transition probabilities should remain invariant as the scene is uniformly scaled, that is, $P(2 \mid 1\,;\, t)$ should remain constant as $|\mathbf{x}_2 - \mathbf{x}_1| \rightarrow \gamma|\mathbf{x}_2 - \mathbf{x}_1|$. Unfortunately, the expressions given previously do not possess this property. However, if the speeds are increased by a factor of γ and the velocity diffusion coefficient is increased by a factor of γ^2, then the expression for $P(2 \mid 1\,;\, t)$ is invariant except for an overall factor of γ^4. Stated differently, $P(2 \mid 1\,;\, t) \rightarrow \gamma^4 P(2 \mid 1\,;\, t)$ when $\dot{\mathbf{x}}_1 \rightarrow \gamma\dot{\mathbf{x}}_1$, $\dot{\mathbf{x}}_2 \rightarrow \gamma\dot{\mathbf{x}}_2$ and $T \rightarrow \gamma^2 T$. While this may at first seem rather *ad hoc*, it is actually quite reasonable—increased displacements require correspondingly higher speeds. Likewise, the diffusion coefficient must increase to effect the equivalent change in particle trajectories. The factor of γ^4 is simply the ratio of sampling volumes in the scaled and unscaled systems (i.e., the Jacobian):

$$P(x_2, y_2, \dot{x}_2, \dot{y}_2 \mid x_1, y_1, \dot{x}_1, \dot{y}_1) =$$
$$\gamma^4 \cdot \int_{-\infty}^{\infty} dx' \int_{-\infty}^{\infty} dy' \int_{-\infty}^{\infty} d\dot{x}' \int_{-\infty}^{\infty} d\dot{y}'\ E(x', \gamma^2\sigma_x^2)\ E(y', \gamma^2\sigma_y^2)\ E(\dot{x}', \gamma^2\sigma_{\dot{x}}^2)\ E(\dot{y}', \gamma^2\sigma_{\dot{y}}^2) \cdot$$
$$p(x_2 - x', y_2 - y', \dot{x}_2 - \dot{x}', \dot{y}_2 - \dot{y}' \mid x_1, y_1, \dot{x}_1, \dot{y}_1)$$

where $E(r', \gamma^2\sigma_r^2) = \exp[-(r'^{\,2}/2\gamma^2\sigma_r^2)]/\sqrt{2\pi\gamma^2\sigma_r^2}$. These considerations lead to the following scale-invariant expressions for $P_{0x}(2 \mid 1\,;\, t)$ and $P_{1x}(2 \mid 1\,;\, t, \xi)$:

$$\begin{aligned}
P_{0x}(2 \mid 1; t) &= \frac{\exp[-(6/\gamma^2 T t^3)(x_{21} - v_x t)^2 (1 - (1 + T t^3/12\sigma_x^2)^{-1})]}{\sqrt{2\pi(\sigma_x^2 + T t^3/12)}} \cdot \\
&\quad \frac{\exp[-(1/2\gamma^2 T t)\dot{x}_{21}^2 (1 - (1 + T t/\sigma_{\dot{x}}^2)^{-1})]}{\sqrt{2\pi(\sigma_{\dot{x}} + T t)}} \cdot \exp(-t/\tau) \\
P_{1x}(2 \mid 1; t, \xi) &= \frac{\exp[-(A_x^2/2\gamma^2 T D)(1 - (1 + T D/\sigma_x^2)^{-1})]}{\sqrt{2\pi(\sigma_x^2 + T D)}} \cdot \\
&\quad \frac{\exp[-(B_x^2/2\gamma^2 T H)(1 - (1 + T H/\sigma_{\dot{x}}^2)^{-1})]}{\sqrt{2\pi(\sigma_{\dot{x}}^2 + T H)}} \cdot \exp(-t/\tau)
\end{aligned}$$

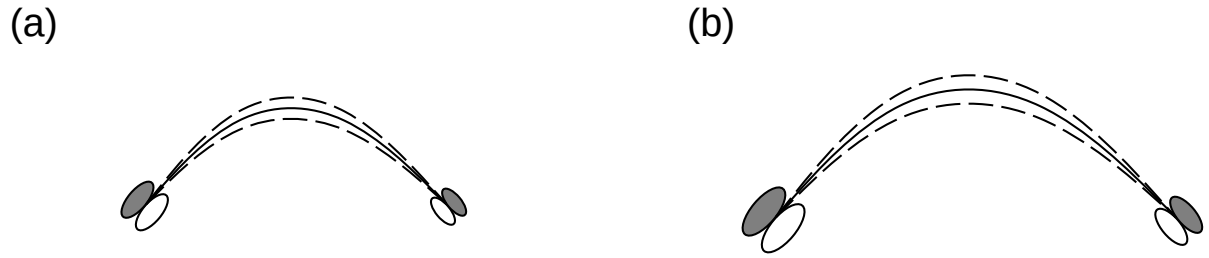

Figure 4: Two completion fields related through a scale transformation. If the distance between the keypoints, $|\mathbf{x}_2 - \mathbf{x}_1|$, and the scale of the filters used to compute the keypoints, $|\dot{\mathbf{x}}_1|$ and $|\dot{\mathbf{x}}_2|$, are increased by a factor of γ, then T must be increased by a factor of γ^2.

From these and the corresponding expressions for the y dimension we obtain $P_0(2 \mid 1; t)$ and $P_1(2 \mid 1; t)$. We note that the γ^2 Jacobian factors in the above expressions are cancelled by γ^2 factors in the denominators.

We must now address the problem of choosing γ. Recall that there are four parameters which define the distribution: T, R_p, ξ_p, and τ. The last three are purely time-like and remain invariant. Only, T, which is proportional to the square of the magnitude of the random impulses, must be scaled by a factor of γ^2. If $|\dot{\mathbf{x}}_1|$ and $|\dot{\mathbf{x}}_2|$ represent the spatial scales of the filters used to compute the keypoints, then letting $\gamma = (|\dot{\mathbf{x}}_1| + |\dot{\mathbf{x}}_2|)/2$ is a natural choice since the larger the velocity, the larger the random impulses which must modify it. The result is that the transition probabilities remain invariant as both the scene *and* the filters are uniformly scaled (see Figure 4).

6 Stochastic Completion Fields

The magnitude of the *stochastic completion field* at $(\eta, \dot{\eta})$ is defined as the probability that a completion, with a distribution of shapes given by $P(2 \mid 1)$, will connect two keypoints via a path through $(\eta, \dot{\eta})$. The stochastic completion field originating in an arbitrary set of n keypoints can (in turn) be expressed as the sum of n^2 pairwise fields. In this section, we describe the problem of computing the completion field for a pair of keypoints, and give example completion fields for a range of speeds.

To accomplish this, we first consider the distribution of contours which begin at the first keypoint, $(\mathbf{x}_1, \dot{\mathbf{x}}_1)$ at time t_1. We then consider the fraction of those contours which pass through the fieldpoint, $(\eta, \dot{\eta})$ at t and then through the second keypoint, $(\mathbf{x}_2, \dot{\mathbf{x}}_2)$ at time t_2 (where $t_2 > t > t_1$). Integrating over all t_1 $(-\infty < t_1 < t)$ and t_2 $(t < t_2 < \infty)$, we find

the relative probability that a completion from $(\mathbf{x}_1, \dot{\mathbf{x}}_1)$ to $(\mathbf{x}_2, \dot{\mathbf{x}}_2)$ includes $(\eta, \dot{\eta})$, giving the value of the stochastic completion field, $C(\eta, \dot{\eta})$. Since the entire history of the contour at t is summarized by $(\eta, \dot{\eta})$ (the velocity fluctuations being independent), the probability of $(\mathbf{x}_1, \dot{\mathbf{x}}_1) \rightarrow (\eta, \dot{\eta}) \rightarrow (\mathbf{x}_2, \dot{\mathbf{x}}_2)$ factors into a product of probabilities for $(\mathbf{x}_1, \dot{\mathbf{x}}_1) \rightarrow (\eta, \dot{\eta})$ and for $(\eta, \dot{\eta}) \rightarrow (\mathbf{x}_2, \dot{\mathbf{x}}_2)$:

$$P((\mathbf{x}_2, \dot{\mathbf{x}}_2, t_2), (\eta, \dot{\eta}, t) \mid (\mathbf{x}_1, \dot{\mathbf{x}}_1, t_1)) = P((\mathbf{x}_2, \dot{\mathbf{x}}_2, t_2) \mid (\eta, \dot{\eta}, t)) \cdot P((\eta, \dot{\eta}, t) \mid (\mathbf{x}_1, \dot{\mathbf{x}}_1, t_1))$$

Figure 5 (a-d) shows four completion fields due to a pair of keypoints positioned on a horizontal line and separated by a distance of 80 pixels. In each subfigure, the orientation of the right keypoint is 130° and the orientation of the left keypoint is 50°. The speeds, γ, in Figure 5 (a-d) are 1,2,4 and 8 respectively. The values of the four parameters defining the contour shape distribution are: $T = 0.0005, \tau = 9.5, \xi_p = 100$ and $R_p = 1.0 \times 10^{-6}$. The completion fields were computed using the expression for $P(2 \mid 1)$ given in Section 4 and using the integral approximations for $P'(2 \mid 1)$ described in Appendix B. Figure 5 (a-d) displays images of size 256×256 where brightness codes the logarithm of the sum of the completion field magnitude evaluated at 36 discrete orientations (i.e., at 10° increments). As the speed is increased, the relative contribution of P_0 and P_1 reverses. This results in a transition from a distribution dominated by smooth contours to a distribution consisting predominantly of straight (or nearly straight) contours containing a single orientation discontinuity. When the distribution is dominated by P_1, the effect of aliasing in orientation becomes evident.

7 Conclusion

In our previous paper[1], we assumed that the statistics of occluded shapes could be modeled by minimally-constrained distributions over all paths. We derived an analytic expression for the shape, salience and sharpness of illusory contours in terms of the characteristic function of the simplest of these distributions (i.e., Gaussian) and applied this expression to well known examples from the visual psychology literature. In this paper, we extended our work in several important directions. First, we have derived a general integral-differential equation including the full spectrum of random impulses and which we believe will be useful for modeling a broad family of shape distributions. We have also derived an analytic expression characterizing the distribution of completion shapes with corners using a mixture of Gaussian and Poisson limiting cases. Finally, we have presented scale-invariant forms for these expressions.

Appendix A: Expected Distributions

For $\mathbf{x}_t = \mathbf{x}_{1t} + \int dt' \mathbf{G}_{t,t'} \mathbf{F}_{t'}$, $\mathbf{F}_{t'}$ stochastic, $\mathbf{F}_t = \sum_{k\ell} \mathbf{f}_k(t - t_{k\ell})$, and $\mathbf{x}_{1t} = \mathbf{x}_1 + \mathbf{G}_{t,t1} \dot{\mathbf{x}}_1$ we desire

$$\Phi(\mathbf{k}_t) = < \exp(i \int dt\ \mathbf{k}_t \cdot \mathbf{x}_t) >_1 = \exp(i \int dt\ \mathbf{k}_t \cdot \mathbf{x}_{1t}) < \exp(i \int dt'\ \mathbf{p}_{t'} \cdot \mathbf{F}_{t'}) >$$

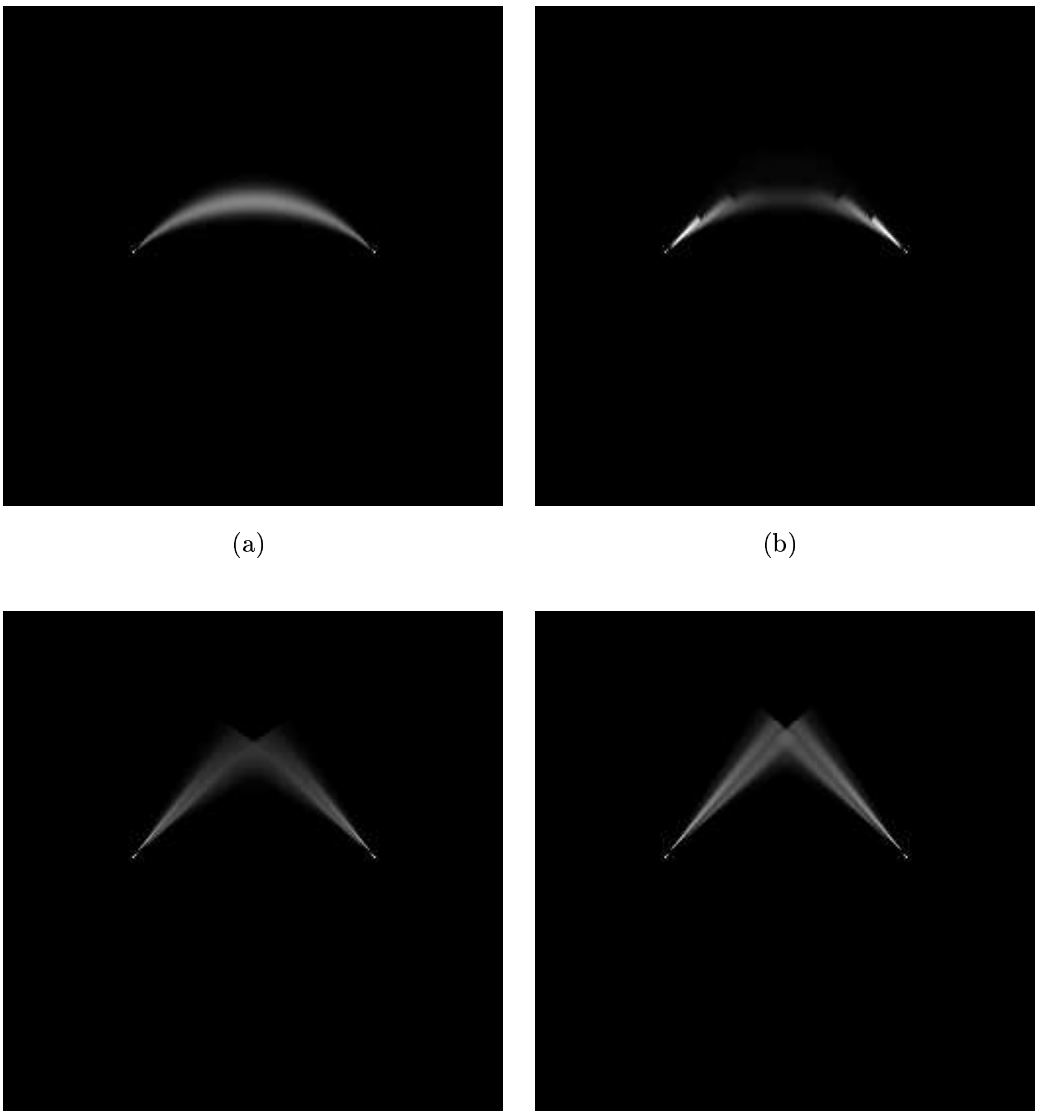

(a) (b)

(c) (d)

Figure 5: Stochastic completion fields (logarithm of magnitude) due to a pair of keypoints positioned on a horizontal line and separated by a distance of 80 pixels. In each subfigure, the orientation of the left keypoint is 130° and the orientation of the right keypoint is 50°. The speeds, γ, in (a-d) are 1,2,4 and 8 respectively. The values of the four parameters defining the contour shape distribution are: $T = 0.0005, \tau = 9.5, \xi_p = 100$ and $R_p = 1.0 \times 10^{-6}$.

with $\mathbf{p}_{t'} = \int dt \mathbf{k}_t \mathbf{G}_{tt'}$. So long as the $t_{k\ell}$'s are independent, we can write

$$\phi(\mathbf{p}_t) =< \exp(i \int dt \mathbf{p}_t \cdot \mathbf{F}_t) >=$$

$$\prod_k \sum_{N_k=0}^{\infty} P_{N_k} (\int dt_k \; R_k(t_k) \exp(i \int dt \; \mathbf{p}_t \mathbf{f}_k(t - t_k))/\lambda_k)^{N_k}$$

where $\lambda_k = \int dt_k R_k(t_k)$ (see [19, 20, 21]). Here P_{N_k} is the probability of N_k events in the time interval of interest, and R_k the average rate of these events. To derive $< \ddot{\mathbf{x}}_{t_2} \delta(\mathbf{x}(t_2) - \mathbf{x}_2) \delta(\dot{\mathbf{x}}(t_2) - \dot{\mathbf{x}}_2) >$, for the integral-differential equation in the text, we must calculate at $\boldsymbol{\eta} = 0$:

$$-i \frac{\partial}{\partial \boldsymbol{\eta}} \int \frac{d\boldsymbol{\kappa}}{(2\pi)^3} e^{-\mathbf{i}\boldsymbol{\kappa} \cdot \mathbf{x}_2} \int \frac{d\boldsymbol{\lambda}}{(2\pi)^3} e^{-i\boldsymbol{\lambda} \cdot \mathbf{x}_2} \Phi(\mathbf{k}_t)$$

for $\mathbf{k}_t = \mathbf{k}_r(t) + \boldsymbol{\eta} \delta''(t - t_2)$ and $\mathbf{k}_r(t) = \boldsymbol{\kappa} \delta(t - t_2) - \boldsymbol{\lambda} \delta'(t - t_2)$. Alternatively, $\mathbf{p}_t = \mathbf{p}_r(t) + \boldsymbol{\eta} \delta(t_2 - t)$. Setting $\mathbf{p}(t) = \mathbf{p}_r(t) = \boldsymbol{\kappa} \mathbf{G}_{t_2,t} + \boldsymbol{\lambda} \partial_{t_2} G_{t_2,t}$ and $\mathbf{k}(t) = \mathbf{k}_r(t)$ results in $P(\mathbf{x}_2, \dot{\mathbf{x}}_2, t_2 \mid \mathbf{x}_1, \dot{\mathbf{x}}_1, t_1)$. Inserting these $\mathbf{p}(t)$ and $\mathbf{k}(t)$ in the expressions for Φ and ϕ above and working out the $\boldsymbol{\eta}$ items, we find for the case that the P_N are Poisson:

$$< \ddot{\mathbf{x}}_{t2} \delta(\mathbf{x}(t_2) - x_2) \delta(\dot{\mathbf{x}}(t_2) - \dot{\mathbf{x}}_2) >=$$

$$\ddot{\mathbf{x}}_{1t} P(\mathbf{x}_2, \dot{\mathbf{x}}_2, t_2 \mid \mathbf{x}_1, \dot{\mathbf{x}}_1, t_1) + \sum_k \int d\xi R_k(\xi) \mathbf{f}_k(t - \xi)$$

$$\cdot P(\mathbf{x}_2 - \int dt' \mathbf{G}_{t,t'} \mathbf{f}_k(t' - \xi), \dot{\mathbf{x}}_2 - \int dt' \partial_t \mathbf{G}_{t,t'} \mathbf{f}_k(t' - \xi), t_2 \mid \mathbf{x}_1, \dot{\mathbf{x}}_1, t_1)$$

We need not take the Poisson limit of P_{N_k}, for we could work directly with Φ and ϕ above, but their representation in an integral-differential equation is unnecessarily complex. We note that the above is valid for general Poisson processes–weak/strong, frequent/infrequent and anything in between. To evaluate $P(2 \mid 1)$ for the Poisson case one simply calculates the above without the $(-i\partial/\partial\boldsymbol{\eta})$ and for $\boldsymbol{\eta} = 0$, proceeding in a manner analogous to [1].

Appendix B: Integral Approximations

The expressions we have derived (thus far) depend on time, i.e., they give the probability that a particle will be at some position and velocity, $(\mathbf{x}_2, \dot{\mathbf{x}}_2)$, at time t given that the particle was observed at some other position and velocity, $(\mathbf{x}_1, \dot{\mathbf{x}}_1)$, at time 0. We refer to this quantity as $P(2 \mid 1; t)$. However, if we are really interested in computing the probability that two boundary fragments are part of the same object, then we are more interested in the integral of $P(2 \mid 1; t)$ over all future times. We refer to this quantity as $P'(2 \mid 1) = \int_0^\infty dt P(2 \mid 1; t)$. To derive an expression for $P'(2 \mid 1)$, we must not only approximate this integral analytically, we must also approximate the integral over the time of the single large scattering event, ξ, in the expression for $P(2 \mid 1; t)$.

To begin, we divide the expression for $P'(2 \mid 1)$ into two terms, I_0 and I_1, and use the method of steepest descent separately on each part. This requires one steepest descent approximation for I_0 and two steepest descent approximations for I_1 (which contains the additional dependency on ξ):

$$\begin{aligned} P'(2 \mid 1) &= \int_0^{t_{max}} dt\ P(2 \mid 1; t) \\ &= \int_0^{t_{max}} dt\ \frac{P_0(2 \mid 1; t) + R_p \int_0^t d\xi P_1(2 \mid 1; t, \xi)}{1 + R_p t} \\ &= \int_0^{t_{max}} dt\ \frac{1}{1 + R_p t} P_0(2 \mid 1; t) + \int_0^{t_{max}} dt'\ \frac{R_p}{1 + R_p t'} \int_0^{t'} d\xi P_1(2 \mid 1; t', \xi) \\ &= I_0 + I_1 \end{aligned}$$

The first integral to be dealt with is that over the time of the single large scattering event:

$$I_R(t') = R_p \int_0^{t'} d\xi P_1(2 \mid 1; t', \xi)$$

Here ξ enters the integrand only through the D and A terms in the expression for $P_1(2 \mid 1; t', \xi)$. A more accurate, steepest-descent approximation would include the ξ-dependence in both. However, since the dependence in the A term dominates the behavior of the integral, we ignore the dependence in the D term in determining the local maximum. We find

$$\begin{aligned} \xi_{opt} &= -\frac{a_x a'_x + a_y a'_y}{{a'_x}^2 + {a'_y}^2} \\ a_x &= x_{21} - \frac{v_x {t'}^2 + \xi_p \dot{x}_2 t'}{t' + \xi_p} \\ a'_x &= \frac{\xi_p \dot{x}_{21}}{t' + \xi_p} \end{aligned}$$

and similarly for a_y and a'_y. The approximate result for the integral is then

$$I_R(t') \approx F_R(\xi_{opt}) R_p P_1(2 \mid 1; t', \xi_{opt})$$

$$F_R(\xi) = \sqrt{2\pi\gamma^2 TD/({a'_x}^2 + {a'_y}^2)}, \quad 0 < \xi < t'$$

When $\xi < 0$ or $\xi > t'$ then we set $F_R = 0$. Of course, I_R is never actually zero. If its behavior for $\xi_{opt} < 0$ or $\xi_{opt} > t'$ is important, we must simply approximate more carefully.

We now face $\int_0^{t_{max}} dt P(2 \mid 1; t)$ where t_{max} is so large that $P(2 \mid 1; t)$ for $t > t_{max}$ is comparatively negligible. There are two integrals with different local optima (i.e., t_{opt} and t'_{opt}). The first integral (which lacks the single large scattering event) is

$$I_0 = \int_0^{t_{max}} dt\ P_0(2 \mid 1; t)/(1 + R_p t)$$

Here the dependence on t in the argument of the exponentials is:

$$-6(g_a/t - g_b/t^2 + g_c/3t^3) - 4\ln t$$

$$\begin{aligned} g_a &= (v_x^2 + v_y^2 + (\dot{x}_{21}^2 + \dot{y}_{21}^2)/12)\gamma^2 T \\ g_b &= 2(x_{21}v_x + y_{21}v_y)/\gamma^2 T \\ g_c &= 3(x_{21}^2 + y_{21}^2)/\gamma^2 T \end{aligned}$$

This argument has a local maximum at $t_{opt} > 0$, where t_{opt} satisfies

$$-2t^3 + 3(g_a t^2 - 2g_b t + g_c) = 0$$

yielding the approximate value for I_0 of

$$I_0 \approx F_0 P_0(2 \mid 1; t_{opt})/(1 + R_p t_{opt})$$

$$F_0 = \sqrt{2\pi t_{opt}^5/(12(g_c - g_b t_{opt}) + 4t_{opt}^3)}$$

If more than one real $t_{opt} > 0$ exists, the one yielding the largest $P_0(2 \mid 1)$ is chosen. Generally, one must take all roots, real and complex, into account. However, for this problem, we found that choosing the largest real root sufficed. The second integral (which includes the single large scattering event) is

$$I_1 = \int_{t_1}^{t_{max}} dt' I_R(t')/(1 + R_p t')$$

If this term is to be important then $\xi_p = (\sigma_v^2/T) >> t'$, in which case the argument of the exponent in I_1 will be maximum for t' close to

$$t'_{opt} = \frac{x_{21}\dot{y}_{21} - y_{21}\dot{x}_{21}}{\dot{x}_1\dot{y}_2 - \dot{x}_2\dot{y}_1}$$

so that

$$I_1 \approx F_1(t'_{opt}) I_R(t'_{opt})/(1 + R_p t'_{opt})$$

$$F_1(t) = \sqrt{2\pi\gamma^2 T D(\dot{x}_{21}^2 + \dot{y}_{21}^2)/(\dot{x}_1\dot{y}_2 - \dot{y}_1\dot{x}_2)^2}$$

for $0 < t'_{opt} < t_{max}$, and $F_1 = 0$ for $t'_{opt} \leq 0$ or $t'_{opt} \geq t_{max}$. As before, F_1 is never really zero. If $0 \leq t_{opt} \leq t_{max}$ and $t'_{opt} < 0$ or $t'_{opt} > t_{max}$, then $I_0 >> I_1$, and I_1 can be ignored. However, if both t_{opt} and t'_{opt} are greater than t_{max}, then t_{max} is too small and should be increased.

Appendix C: Constant Speed Case

In this Appendix, we give expressions for the special case of contours which have the same initial and final speed. Our intention is to approximate the distribution of contours described by Mumford[4] and Williams and Jacobs[6]. This is the distribution of trajectories in the

plane traced by particles travelling with constant speed in directions given by Brownian motions. For equal initial and final speeds, the convolution with broadening functions (employed as an anti-aliasing measure) is over position and direction, not position and velocity. Consequently, the Jacobian (i.e., the ratio of sampling volumes in the scaled and unscaled systems) is γ^2 (not γ^4):

$$P(x_2, y_2, \theta_2 \mid x_1, y_1, \theta_1) =$$

$$\gamma^2 \cdot \int_{-\infty}^{\infty} dx' \int_{-\infty}^{\infty} dy' \int_{-\infty}^{\infty} d\theta' \; E(x', \gamma^2\sigma_x^2) \; E(y', \gamma^2\sigma_y^2) \; E(\theta', \sigma_\theta^2) \; p(x_2 - x', y_2 - y', \theta_2 - \theta' \mid x_1, y_1, \theta_1)$$

where $E(r', \gamma^2\sigma_r^2) = \exp[-(r'^{\,2}/2\gamma^2\sigma_r^2)]/\sqrt{2\pi\gamma^2\sigma_r^2}$. This leads to the following scale-invariant expressions for $P_0(2 \mid 1\,;\, t)$ and $P_1(2 \mid 1\,;\, t, \xi)$:

$$\begin{aligned}
P_0(2 \mid 1; t) \;=\; & \frac{\exp[-(6/\gamma^2 T t^3)(x_{21} - v_x t)^2 (1 - (1 + Tt^3/12\sigma_x^2)^{-1})]}{\sqrt{2\pi(\sigma_x^2 + Tt^3/12)}} \cdot \\
& \frac{\exp[-(6/\gamma^2 T t^3)(y_{21} - v_y t)^2 (1 - (1 + Tt^3/12\sigma_y^2)^{-1})]}{\sqrt{2\pi(\sigma_y^2 + Tt^3/12)}} \cdot \\
& \frac{\exp[-(1/2\gamma^2 T t)(\dot{x}_{21}^2 + \dot{y}_{21}^2)(1 - (1 + Tt/\sigma_\theta^2)^{-1})]}{\sqrt{2\pi(\sigma_\theta^2 + Tt)}} \cdot \exp(-t/\tau) \\
P_1(2 \mid 1; t, \xi) \;=\; & \frac{\exp[-(A_x^2/2\gamma^2 TD)(1 - (1 + TD/\sigma_x^2)^{-1})]}{\sqrt{2\pi(\sigma_x^2 + TD)}} \cdot \\
& \frac{\exp[-(A_y^2/2\gamma^2 TD)(1 - (1 + TD/\sigma_y^2)^{-1})]}{\sqrt{2\pi(\sigma_y^2 + TD)}} \cdot \\
& \frac{\exp[-(1/2\gamma^2 TH)(\dot{x}_{21}^2 + \dot{y}_{21}^2)(1 - (1 + TH/\sigma_\theta^2)^{-1})]}{\sqrt{2\pi(\sigma_\theta^2 + TH)}} \cdot \exp(-t/\tau)
\end{aligned}$$

where $\dot{x}_1 = \gamma\cos\theta_1, \dot{x}_2 = \gamma\cos\theta_2, \dot{y}_1 = \gamma\sin\theta_1$ and $\dot{y}_2 = \gamma\sin\theta_2$. As before, the Jacobian factor is cancelled by equal factors in the denominators of the above expressions. Finally, we note that for the constant speed case, there is a small change in the integral approximations described in Appendix B. The optimum time, t_{opt}, in the steepest descent approximation of I_0 now solves:

$$-\frac{7}{4}t^3 + 3(g_a t^2 - 2g_b t + g_c) = 0$$

The integral approximations are otherwise unchanged.

References

[1] Thornber, K.K. and L.R. Williams, Analytic Solution of Stochastic Completion Fields, *Biological Cybernetics* **75**, pp. 141-151, 1996.

[2] Thornber, K.K. and L.R. Williams, Scale, Orientation and Discontinuity as Emergent Properties of Illusory Contour Shape, *Neural Information Processing Systems (NIPS '98)*, Denver, CO, 1998.

[3] Williams, L.R., and K.K. Thornber, A Comparison of Measures for Detecting Natural Shapes in Cluttered Backgrounds, *Proc. of the 5th European Conf. on Computer Vision (ECCV '98)*, Freiburg, Germany, 1998.

[4] Mumford, D., Elastica and Computer Vision, *Algebraic Geometry and Its Applications*, Chandrajit Bajaj (ed.), Springer-Verlag, New York, 1994.

[5] Cox, I.J., Rehg, J.M. and Hingorani, S., A Bayesian Multiple Hypothesis Approach to Edge Grouping and Contour Segmentation, *Intl. Journal of Computer Vision* **11**, pp. 5-24, 1993.

[6] Williams, L.R., and D.W. Jacobs, Stochastic Completion Fields: A Neural Model of Illusory Contour Shape and Salience, *Neural Computation* **9**, pp. 837-858, 1997.

[7] Horn, B.K.P., The Curve of Least Energy, MIT AI Lab Memo No. 612, MIT, Cambridge, Mass., 1981.

[8] Kass, M., Witkin, A. and Terzopolous, D., Snakes: Active Minimum Energy Seeking Contours, *Proc. of the First Intl. Conf. on Computer Vision (ICCV)*, London, England, pp. 259-268, 1987.

[9] Kanizsa, G., *Organization in Vision*, Praeger, New York, 1979.

[10] Sambin, M., Angular Margins without Gradients, *Italian Journal of Psychology* **1**, pp. 355-361, 1974.

[11] Mumford, D. and Shah, J., Boundary Detection by Minimizing Functionals, *Proc. IEEE Conf. on Comp. Vision and Pattern Recognition (CVPR)*, 1985.

[12] Blake, A., The Least Disturbance Principle and Weak Constraints, *Pattern Recognition Letters* **1**, pp. 393-399, 1983.

[13] Geman, S. and D. Geman, Stochastic Relaxation, Gibbs Distributions, and Bayesian Restoration of Images, *IEEE Trans. Pattern Analysis and Machine Intelligence* **6**, pp. 721-741, 1984.

[14] Marroquin, J., Surface Reconstruction Preserving Discontinuities, MIT AI Lab Memo No. 792, MIT, Cambridge, MA, 1984.

[15] Grimson, W.E.L., and Pavlidis, T., Discontinuity Detection for Visual Surface Reconstruction, *Computer Vision, Graphics, and Image Processing* **30**, pp. 316-330, 1985.

[16] Terzopolous, D., Computing Visible Surface Representations, MIT AI Lab Memo No. 612, MIT, Cambridge, MA, 1985.

[17] Belheumer, P.N., Bayesian Models for Reconstructing the Scene Geometry in a Pair of Stereo Images, *Proc. Conf. Information Sciences and Systems*, Johns Hopkins University, Baltimore, MD, 1993.

[18] Heitger, R. and von der Heydt, R., A Computational Model of Neural Contour Processing, Figure-ground and Illusory Contours, *Proc. of 4th Intl. Conf. on Computer Vision*, Berlin, Germany, 1993.

[19] Feynman, R.P. and A.R. Hibbs, *Quantum Mechanics and Path Integrals*, New York, McGraw Hill, 1965.

[20] Thornber, K.K., Treatment of Microscopic Fluctuations in Noise Theory, *BSTJ* **53**, pp. 1041-1078, 1974.

[21] Thornber, K.K., A New Approach for Treating Fluctuations in Noise Theory, *J. Appl. Phys.* **46**, pp. 2781-2787, 1975.